AEDC-TR-71-173

Cy 2

INVESTIGATION OF THE AEROELASTIC STABILITY OF THIN CYLINDRICAL SHELLS AT SUBSONIC MACH NUMBERS

Warren E. White

ARO, Inc.

November 1971

PROPULSION WIND TUNNEL FACILITY
ARNOLD ENGINEERING DEVELOPMENT CENTER
AIR FORCE SYSTEMS COMMAND
ARNOLD AIR FORCE STATION, TENNESSEE

NOTICES

When U. S. Government drawings specifications, or other data are used for any purpose other than a definitely related Government procurement operation, the Government thereby incurs no responsibility nor any obligation whatsoever, and the fact that the Government may have formulated, furnished, or in any way supplied the said drawings, specifications, or other data, is not to be regarded by implication or otherwise, or in any manner licensing the holder or any other person or corporation, or conveying any rights or permission to manufacture, use, or sell any patented invention that may in any way be related thereto.

Qualified users may obtain copies of this report from the Defense Documentation Center.

References to named commercial products in this report are not to be considered in any sense as an endorsement of the product by the United States Air Force or the Government.

INVESTIGATION OF THE AEROELASTIC STABILITY OF THIN CYLINDRICAL SHELLS AT SUBSONIC MACH NUMBERS

Warren E. White
ARO, Inc.

FOREWORD

The work reported herein was done at the request of the Aerospace Engineering Department of the University of Texas for the Air Force Office of Scientific Research (AFOSR), Air Force Systems Command (AFSC), under Program Element 61102F/9F82, Task 01.

The results of the test presented were obtained by ARO, Inc. (a subsidiary of Sverdrup & Parcel and Associates, Inc.), contract operator of the Arnold Engineering Development Center (AEDC), AFSC, Arnold Air Force Station, Tennessee, under Contract F40600-72-C-0003. The test was conducted from May 5 through 9, 1971, under ARO Project No. PB0189. The manuscript was submitted for publication on July 2, 1971.

This technical report has been reviewed and is approved.

George F. Garey
Lt Colonel, USAF
AF Representative, PWT
Directorate of Test

Duncan W. Rabey, Jr.
Colonel, USAF
Director of Test

ABSTRACT

Boundary-layer and static-pressure data were obtained over a rigid pressure shell at Mach numbers from 0.6 to 0.9 and Reynolds numbers per foot from 0.3 x 10^6 to 5.3 x 10^6. These data were obtained with and without the addition of air injected into the boundary layer through a circular slot upstream of the test shell. Static aeroelastic characteristics of thin cylindrical shells were obtained at Mach number 0.9 without the use of boundary-layer control and without shell axial-force loading. An aeroelastic buckling failure was induced on all three shells by reducing the cavity pressure. Flutter of the shell was not encountered during the test.

CONTENTS

APPENDIXES

NOMENCLATURE

C_p	Pressure coefficient, $(p - p_\infty)/q_\infty$
E	Young's modulus of elasticity, 14×10^6, psi
$\overline{F}$	Flutter parameter, $\left(\frac{q_\infty}{E\sqrt{\lvert M_\infty^2 - 1 \rvert}}\right)^{1/3}\left(\frac{R}{h}\right)$
h	Shell thickness, in.
L	Shell reference length, 1.333 ft
M_L	Local Mach number
M_∞	Free-stream Mach number
p	Local pressure on model surface, psfa
p_a	Pressure in axial bladder, psia
p_c	Cavity pressure beneath the shell, psia
Δp_c	Differential pressure across test shell $(p_c - p_\infty)$, psi
p_{t_∞}	Free-stream total pressure. psfa
p_∞	Free-stream static pressure, psfa
q_∞	Free-stream dynamic pressure, psf
R	Shell radius, 8.00 in.

r	Radius of ogive nose, in.
Re/ft	Reynolds number per foot, V_∞/υ_∞
V_∞	Free-stream velocity, ft/sec
$\dot{\omega}$	Weight flow into boundary layer, lb/sec
x	Distance from the forward edge of the test shell, ft
y	Distance measured normal to the model surface, in.
υ_∞	Free-stream kinematic viscosity, ft^2/sec
ϕ	Rotational angle measured on the model, Fig. 5, deg

SECTION I
INTRODUCTION

An investigation of the aeroelastic stability characteristics of thin cylindrical shells was conducted in the transonic Propulsion Wind Tunnel (16T). The test was divided into a pressure phase and a flutter phase.

The purpose of the pressure phase was to determine boundary-layer profiles and static-pressure distributions over a rigid shell with and without the addition of air injected into the boundary layer at Mach numbers from 0.60 to 0.95.

The objective of the flutter phase was to determine the flutter characteristics of three flexible cylindrical shells as influenced by shell thickness and shell cavity pressure at Mach number 0.90.

Earlier shell flutter tests were conducted in the Propulsion Wind Tunnels (16T) and (16S) and have been documented in Refs. 1, 2, and 3.

SECTION II
APPARATUS

2.1 WIND TUNNEL

Tunnel 16T is a variable density wind tunnel capable of operation at Mach numbers from 0.20 to 1.60. The tunnel is equipped with a plenum evacuation system, and the test section is formed by fixed, parallel top and bottom perforated walls and perforated, variable angle sidewalls.

Details of the perforated walls and the location of the model and support strut in the test section are shown in Fig. 1 (Appendix I). A photograph of the model installed in Tunnel 16T is presented in Fig. 2.

2.2 TEST ARTICLE

A detailed drawing of the ogive-cylinder model is shown in Fig. 3. The model has a 3-cal circular arc ogive nose with an 18.9-deg semivertex angle, a fineness ratio of approximately 8, and a maximum diameter of 16 in. The model is composed of three basic sections: the nose cone, center section, and the aft or base supporting structure. The primary function of the nose cone is to provide a uniform flow and static-pressure field over the test shell and to support the boundary-layer control equipment. The center section supports either the rigid pressure shell or thin flexible flutter shell and its associated instrumentation, whereas the base section attaches the model to the supporting sting.

Details of the pressure and flutter shells are presented in Figs. 4 and 5. The static pressure shell was constructed from 0.080-in.-thick copper sheet with four rows of orifices along the shell (Fig. 4a). Additional orifices were located on the model as shown in Fig. 3.

Three boundary-layer rakes were used: one fixed, one remotely adjustable vertically, and one remotely adjustable longitudinally. Rakes 1 and 2 were located at model station 114.25, whereas the longitudinally adjustable rake was remotely variable between stations 98.25 and 114.25. The fixed and adjustable rakes are illustrated in Figs. 6 and 7.

The flutter shells were thin-walled monocoque circular cylinders made by an electroplating process. The shell thicknesses were 0.0027, 0.0030, and 0.0032 in., as shown in Table I (Appendix II). These shells were soldered to two copper end rings which were machined to fit smoothly against radial and axial bladders. These bladders were located inside the fore and aft edges of the center section (Fig. 5). The internal pressure in the axial bladders could be remotely controlled to produce an axial buckling load (longitudinally compressive) in the shell.

2.3 INSTRUMENTATION

2.3.1 Pressure Phase

Twenty-four static-pressure orifices were uniformly distributed along four rays 90 deg apart on the shell, and nine orifices were located elsewhere on the model as shown in Fig. 3. Three static-pressure orifices were located internally in the boundary-layer control duct, and one orifice was installed in the cavity beneath the pressure shell. All the pressure orifices were connected to pressure transducers which were located in the tunnel plenum chamber. All transducer outputs were fed to analog-to-digital converters and then to a digital computer.

Twenty-nine total pressures were measured from the three boundary-layer rakes (Fig. 6). Rakes 1 and 3 had static-pressure probes on the rakes, but Rake 2 used a static referenced pressure measured on the model surface.

2.3.2 Flutter Phase

A photograph of the model instrumentation used in the flutter phase is presented in Fig. 8. The model displacement sensors were mutual-inductance proximity transducers designed to sense both static and dynamic displacements of a point on the shell surface without mechanical contact (Ref. 4). Sensor 1 could translate fore and aft from 10 to 85 percent of the shell length at a speed of 25 in./min. Both sensors 1 and 2 could rotate circumferentially under the shell from 0 through 270 deg. Sensor 3, which is covered in the photograph, was fixed in position and used as a reference sensor to assist in mode shape identification through phase-angle measurements between this sensor and the two moving sensors.

The signals from these sensors were amplified and fed into two magnetic tape recorders and a direct-writing oscillograph. A dual-beam oscilloscope was used for continuous monitoring of shell motion. The inputs to the oscilloscope could be varied from one sensor to another as it became necessary to compare the phasing and relative amplitude of the three sensors. The magnetic tape recorders were sometimes run continuously when the shell sensor signals appeared to coalesce in frequency and increase in amplitude.

SECTION III
TEST PROCEDURES

3.1 PRESSURE PHASE

Boundary-layer profiles and static-pressure distributions were obtained at Mach numbers from 0.60 to 0.95 at Reynolds numbers per foot from approximately 0.30×10^6 to 5.30×10^6. Air was blown into the boundary layer through a circumferential slot ahead of the test shell.

The boundary-layer control (BLC) system was operated to provide nominal weight flows of 0, 0.20, 0.45, and 0.80 lb/sec.

3.2 FLUTTER PHASE

For the three flexible shell configurations tested, the Mach number was established at 0.90 and at a low dynamic pressure level. The dynamic pressure was slowly increased in increments while maintaining a constant Mach number until a designated limit or tunnel maximum was obtained. After the desired total pressure level was reached, model cavity pressure was reduced until flutter or static aeroelastic buckling occurred. Internal cavity pressure was varied only when the tunnel conditions were constant.

3.3 PRECISION OF MEASUREMENTS

The magnitude of the uncertainties involved in the tunnel conditions is estimated to be as follows:

Mach Number	±0.003
Total Pressure	±5 psf
Dynamic Pressure	±0.5 percent
Total Temperature	±5°F

The Mach number error does not include the deviation from the mean value in the region of the model. The maximum variation in Mach number on the tunnel centerline in the vicinity of the model was ±0.004.

The magnitude of the uncertainties in shell frequency measurement, based on repeatability during the wind-off calibrations, and the accuracies in determining shell flutter frequencies from oscillograph records of the variable inductance sensors are estimated to be 2 Hz.

SECTION IV
RESULTS AND DISCUSSION

4.1 PRESSURE PHASE

The pressure coefficients shown in Fig. 9 were computed from measurements at the static-pressure orifices in the rigid test shell for Mach numbers 0.60, 0.90, and 0.95, respectively. The large pressure increases near the aft end of the shell in the 0- and 270-deg rays are attributable to the influence of instrumentation enclosures on the sting aft of the model (see Fig. 2) and the location of the three boundary-layer rakes. The maximum variation in pressure coefficient across the shell was from approximately 0 to 0.064 along the shell 270-deg ray.

Representative boundary-layer profiles obtained with the vertical adjustable rake are presented in Fig. 10 for Mach numbers of 0.6, 0.8, and 0.9 using boundary-layer control blowing rates that varied from 0 to 0.80 lb/sec. The effects of varying Reynolds number per foot for different boundary-layer blowing rates are shown in Fig. 11. The boundary-layer rake was located aft of the test shell at model station 114.25 in. and traversed vertically from 0 to 1.13 in. above the shell. Insignificant changes in the turbulent boundary-layer profiles resulted from mass addition of air injected into the boundary layer.

4.2 FLUTTER PHASE

Test conditions and ranges of variation for the control condition are shown in Table I (Appendix II). Three shells with thicknesses of 0.0027, 0.0030, and 0.0032 in. were tested. Static aeroelastic buckling characteristics were obtained at only Mach number 0.90. Aeroelastic buckling failures were induced in all three shells by reducing the model cavity pressure while maintaining a constant Mach number and total pressure. The shell axial load was zero through this phase of the test. High-speed motion pictures were obtained of two of three shell configurations. Some of the sequence frames which depict the shell failures are presented in Fig. 12. The shell failure that was not recorded on film occurred earlier than anticipated because of a possible weak bond between the shell and the forward retainer ring. Shell panel flutter was not encountered during this test.

REFERENCES

1. Perkins, T. M. and Brice, T. R. "An Investigation of the Aeroelastic Stability of Thin Cylindrical Shells at Transonic Mach Numbers." AEDC-TR-66-93 (AD632829), May 1966.

2. Brice, T. R. "Aeroelastic Stability Tests of Thin Cylindrical Shells at Supersonic Speeds." AEDC-TR-68-79 (AD830407), April 1968.

3. White, Warren E. "Aeroelastic Stability Tests of Thin Cylindrical Shells at Supersonic Speeds (Follow-On Test)." AEDC-TR-69-98 (AD851095), April 1969.

4. Horn, W., Barr, G., Carter, L., and Stearman, R. "Recent Contributions to Experiments on Cylindrical Shell Panel Flutter." AIAA/ASME Twelfth Structures, Structural Dynamics and Material Conference, Anaheim, California/April AIAA Paper No. 71-328, April 1971.

APPENDIXES

I. ILLUSTRATIONS
II. TABLE

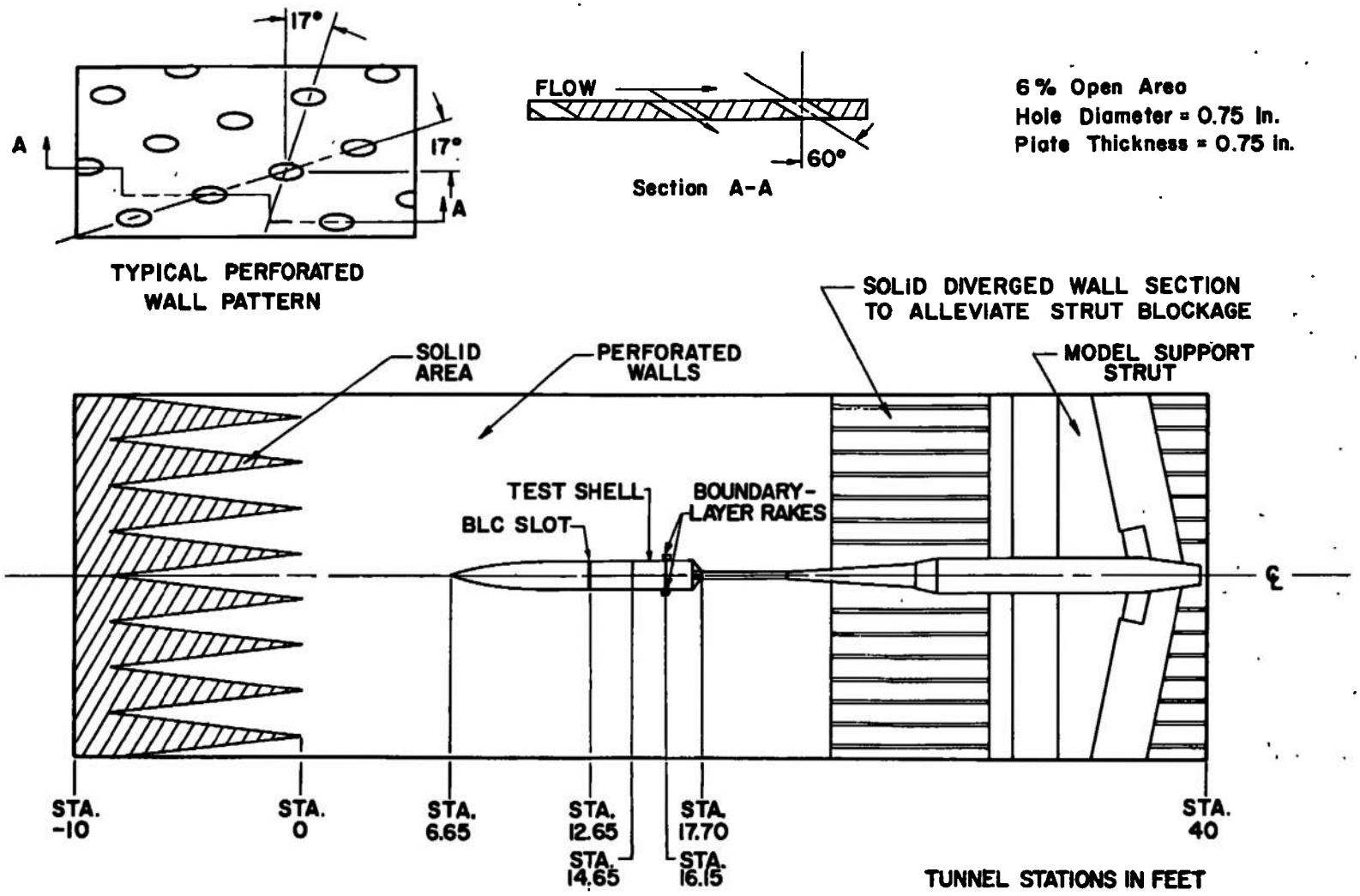

Fig. 1 Schematic of Model Installation

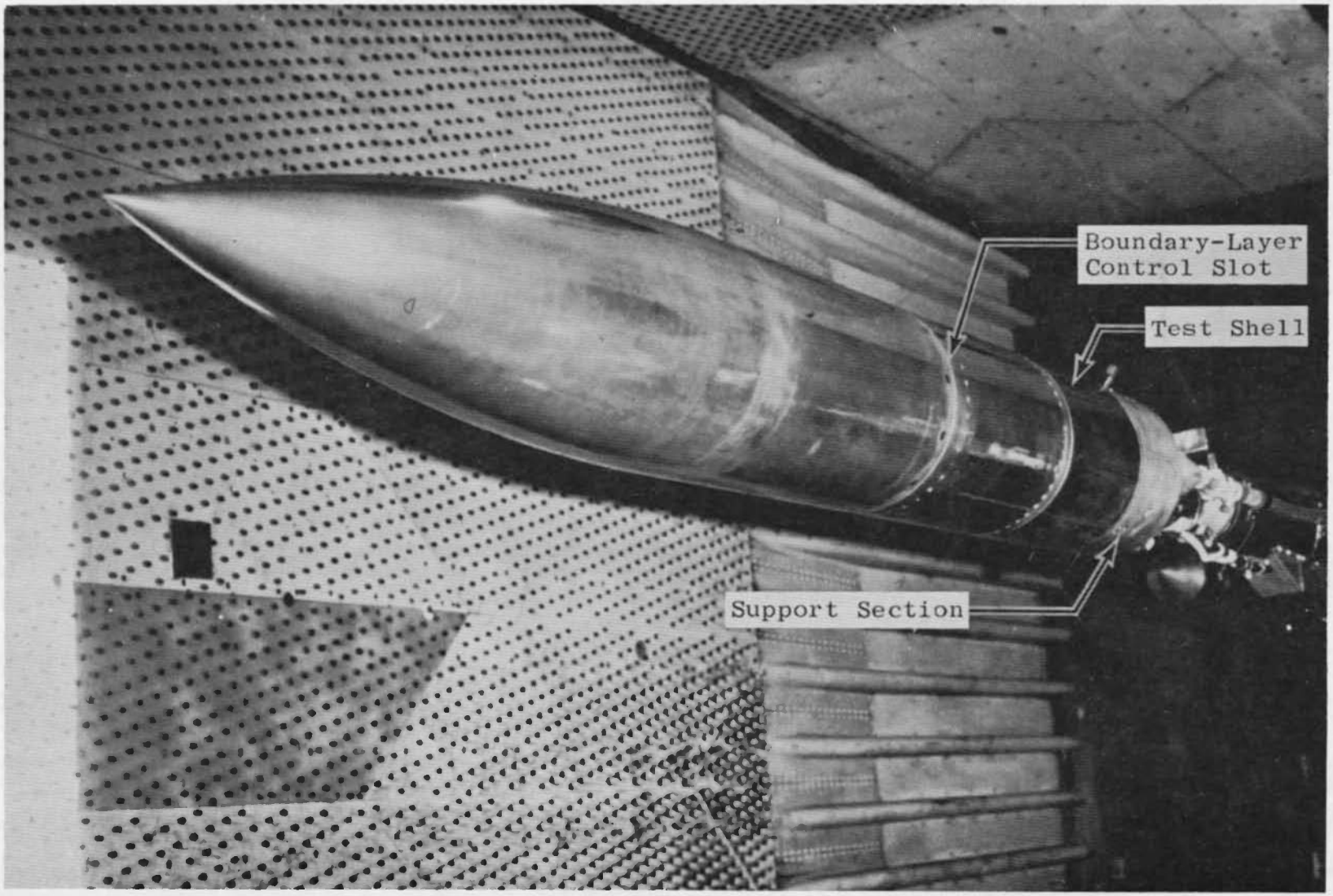

Fig. 2 Photograph of Model Installed in Test Section

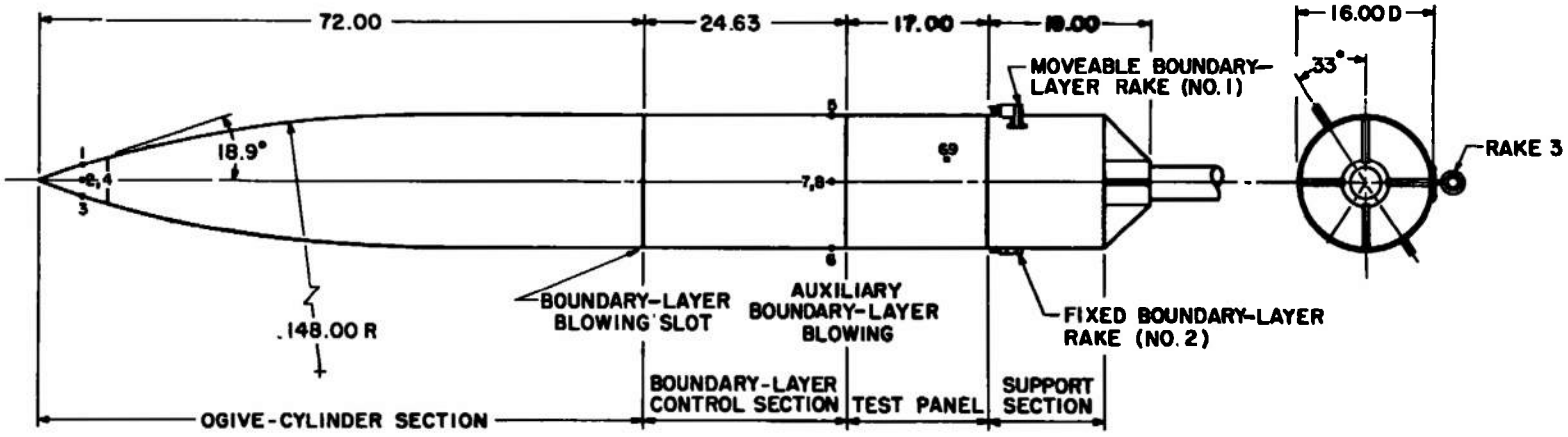

ALL DIMENSIONS IN INCHES.

Fig. 3 Details of Ogive-Cylinder Model

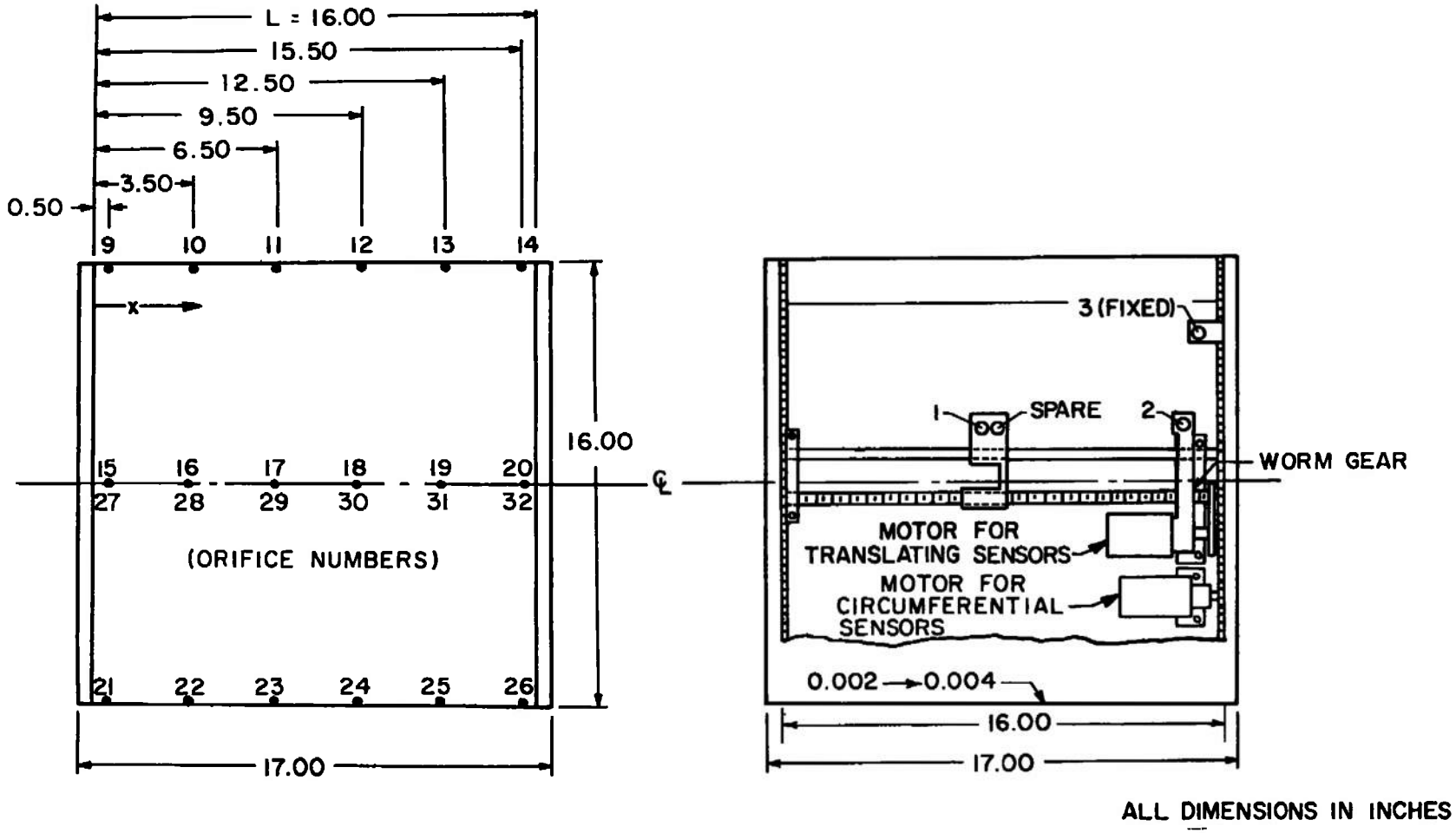

a. Rigid Pressure Shell

b. Flexible Flutter Shell

Fig. 4 Details of Test Shell Instrumentation

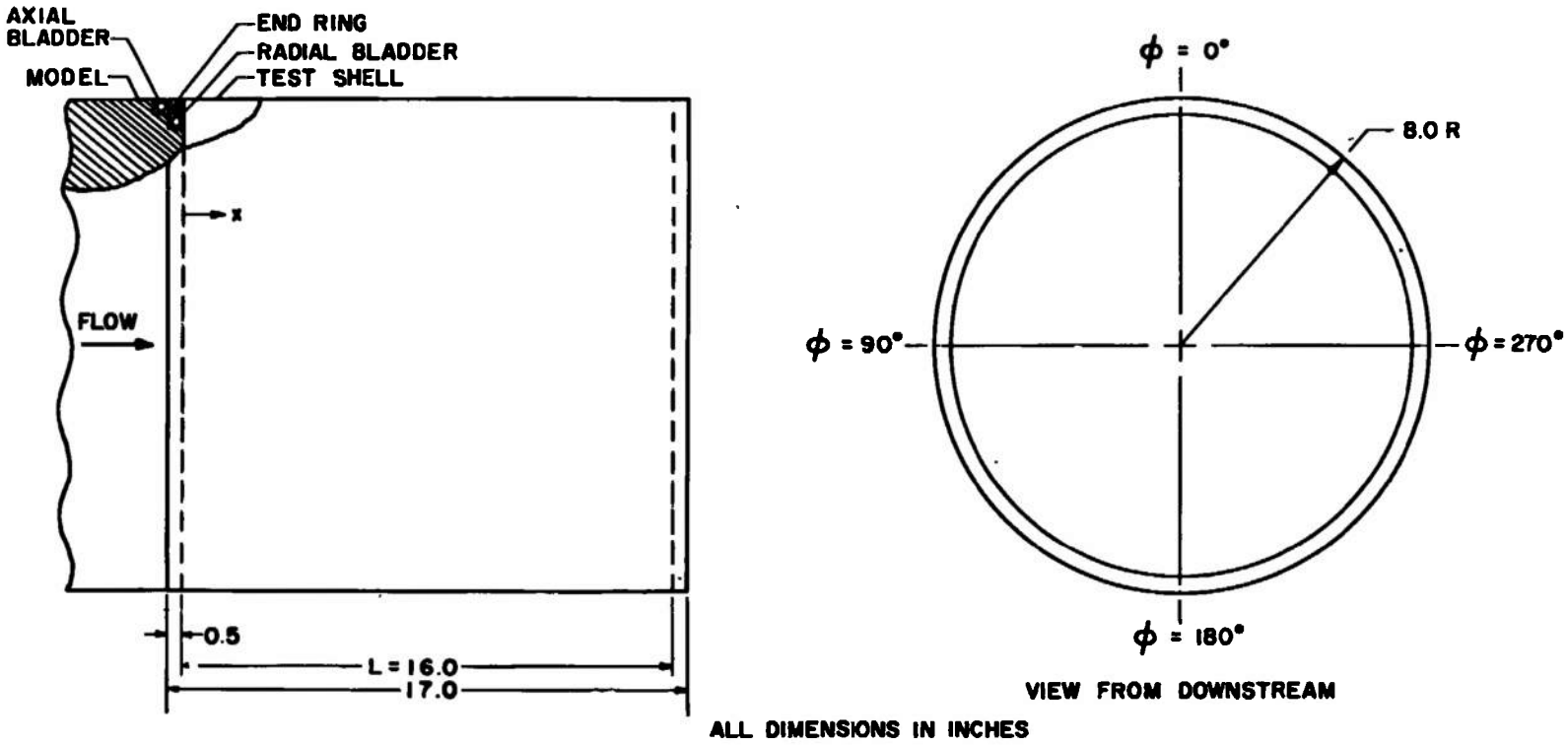

Fig. 5 Details of the Test Shell

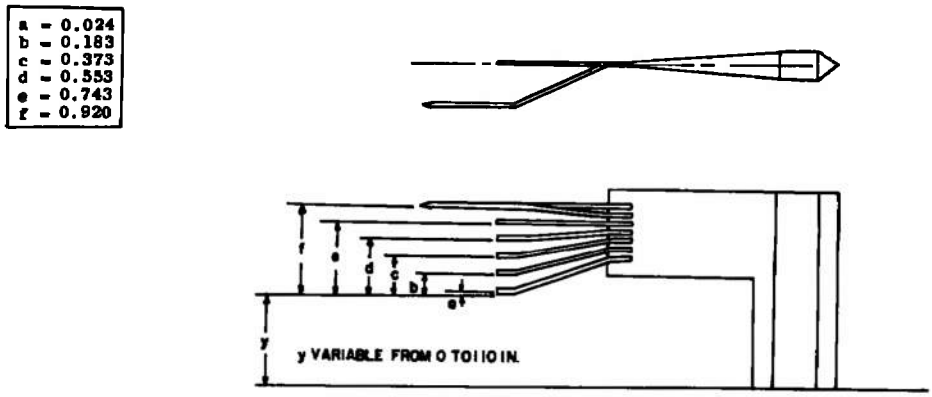

a. Rake 1

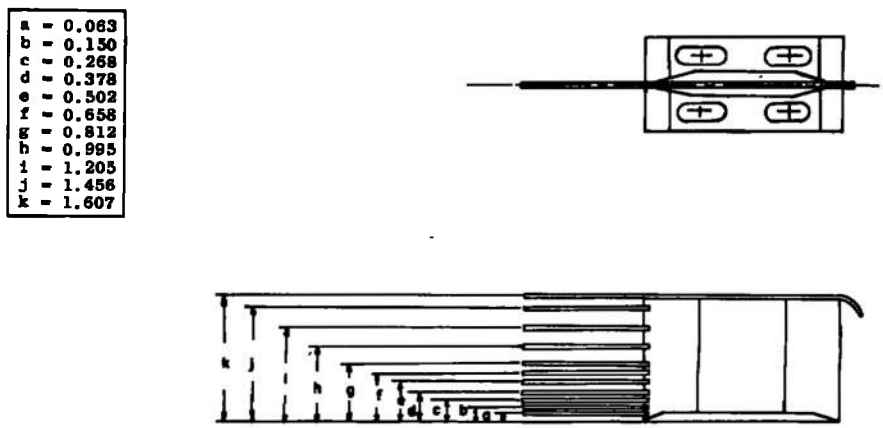

b. Rake 2

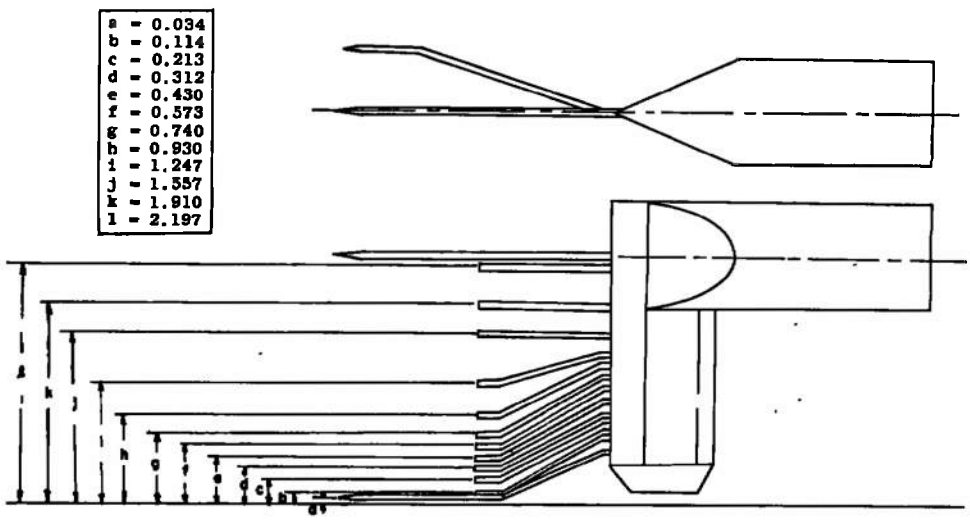

c. Rake 3

Fig. 6 Details of the Boundary-Layer Rakes

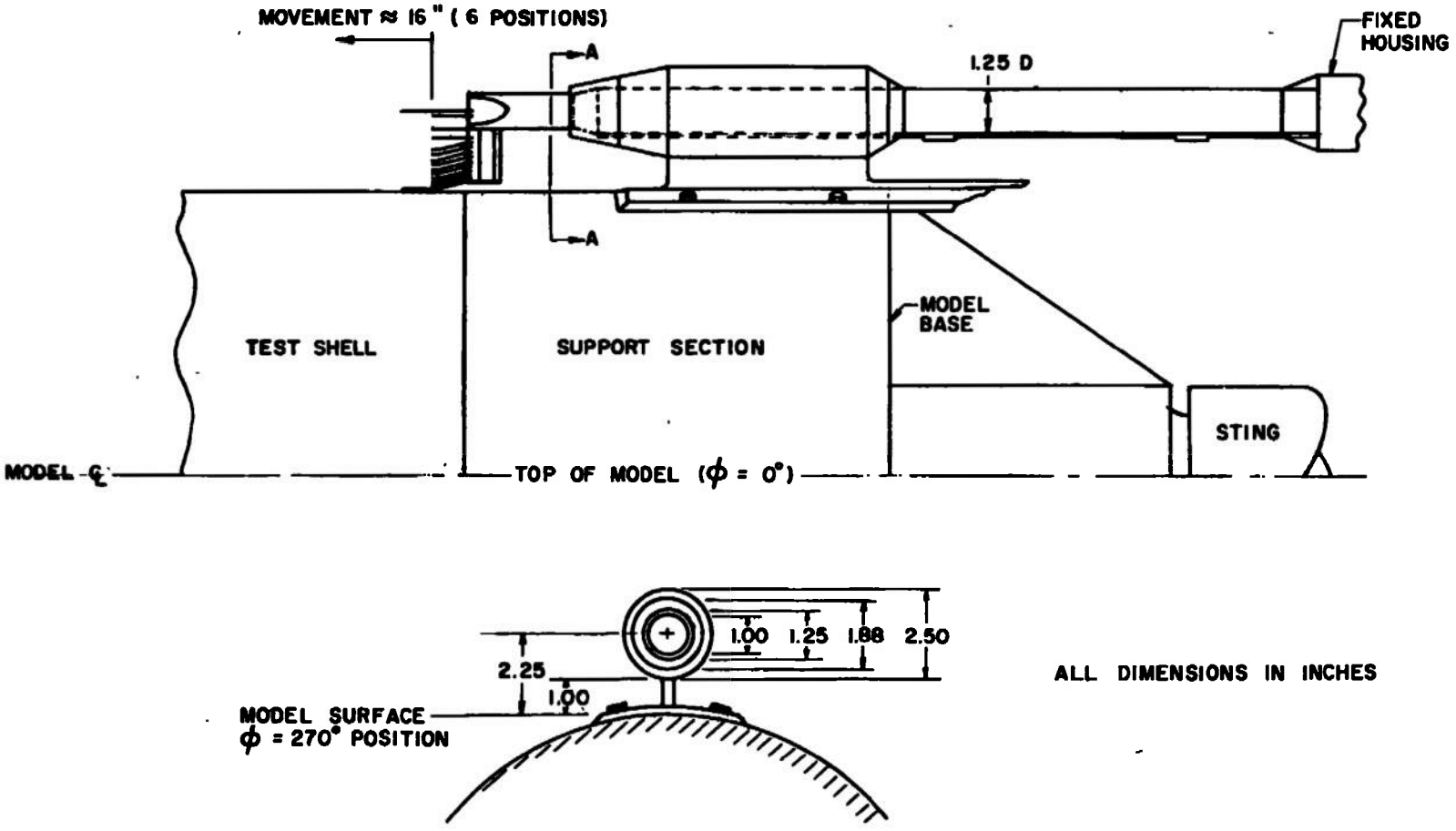

Fig. 7 Details of the Traversing Rake (Rake 3)

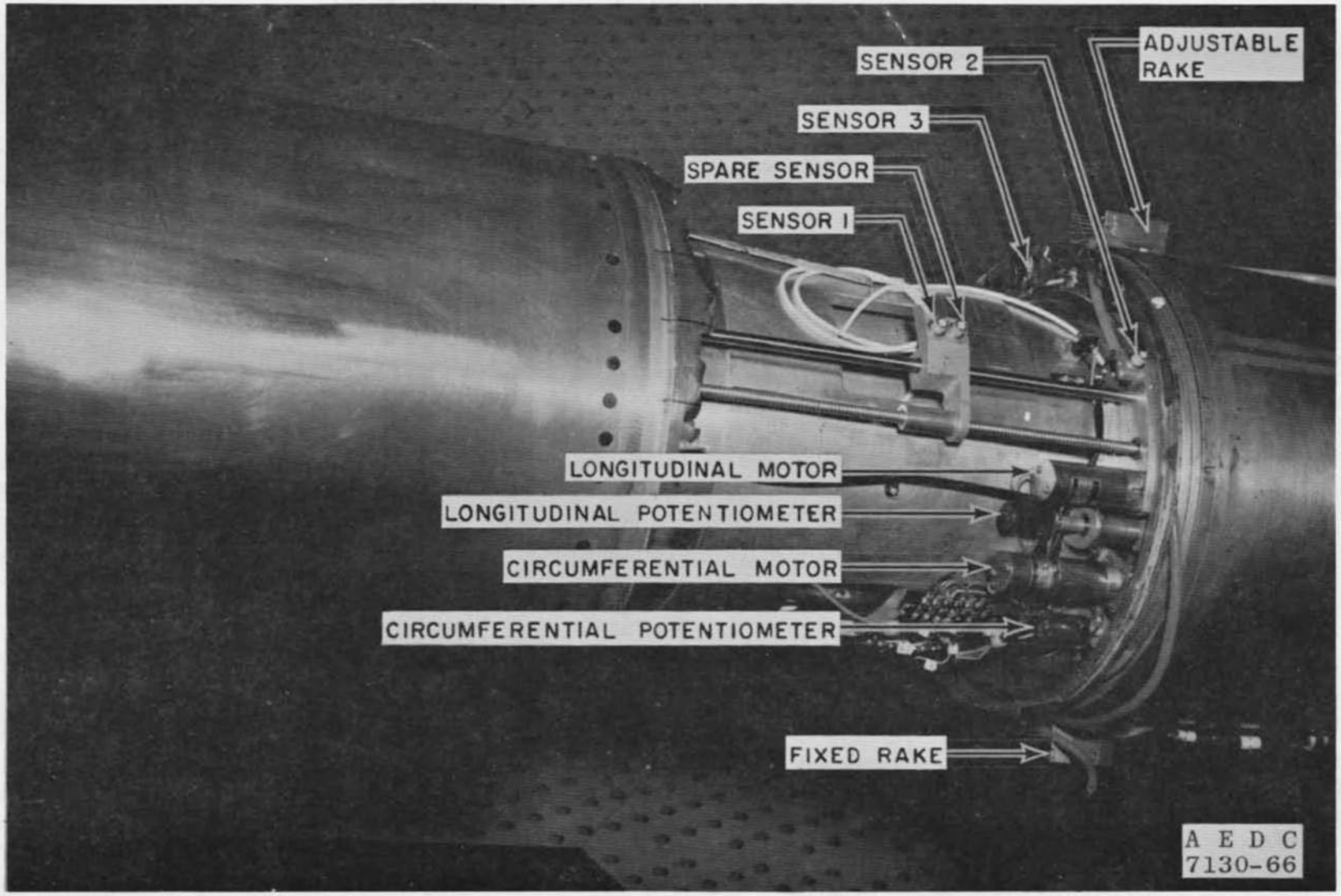

Fig. 8 Photograph of Model Instrumentation Used during Flutter Phase

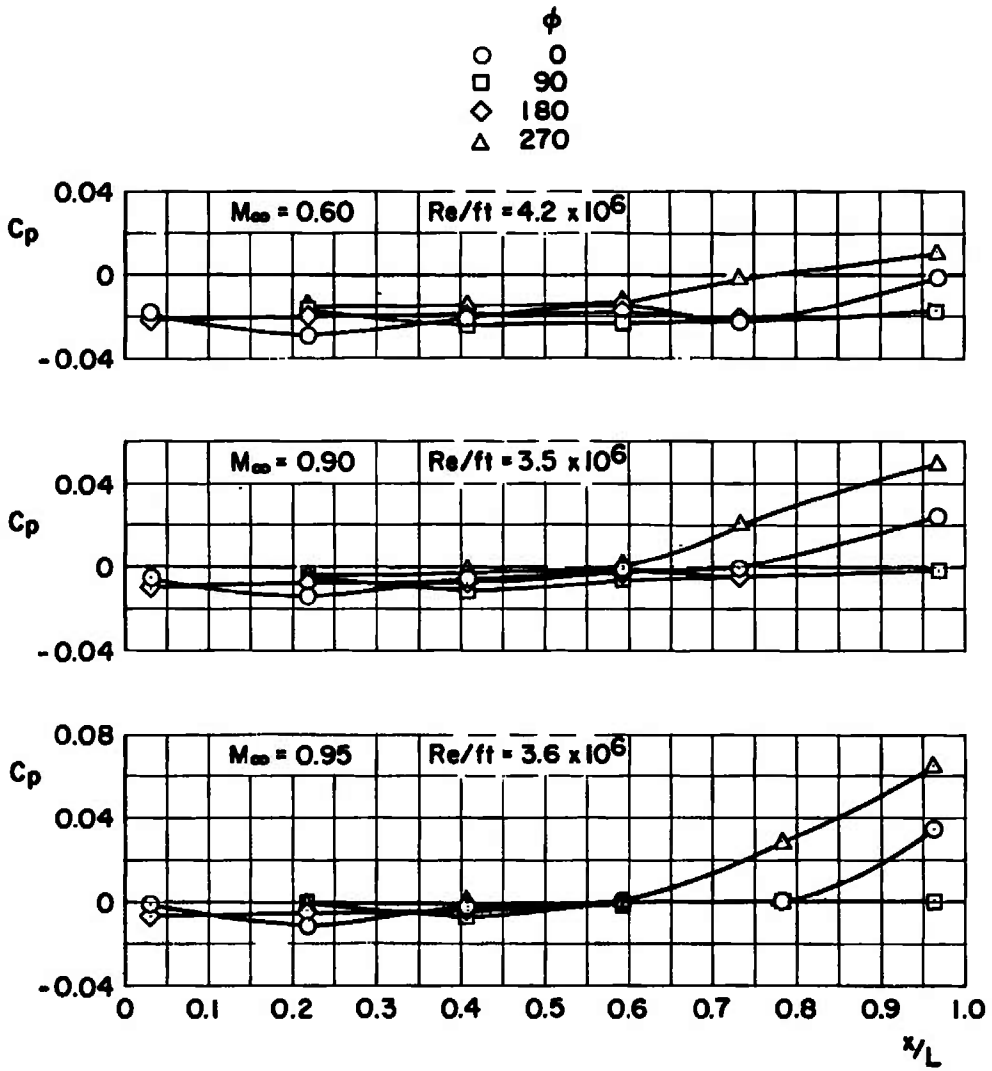

Fig. 9 Variation of Pressure Coefficient along the Rigid Test Shell

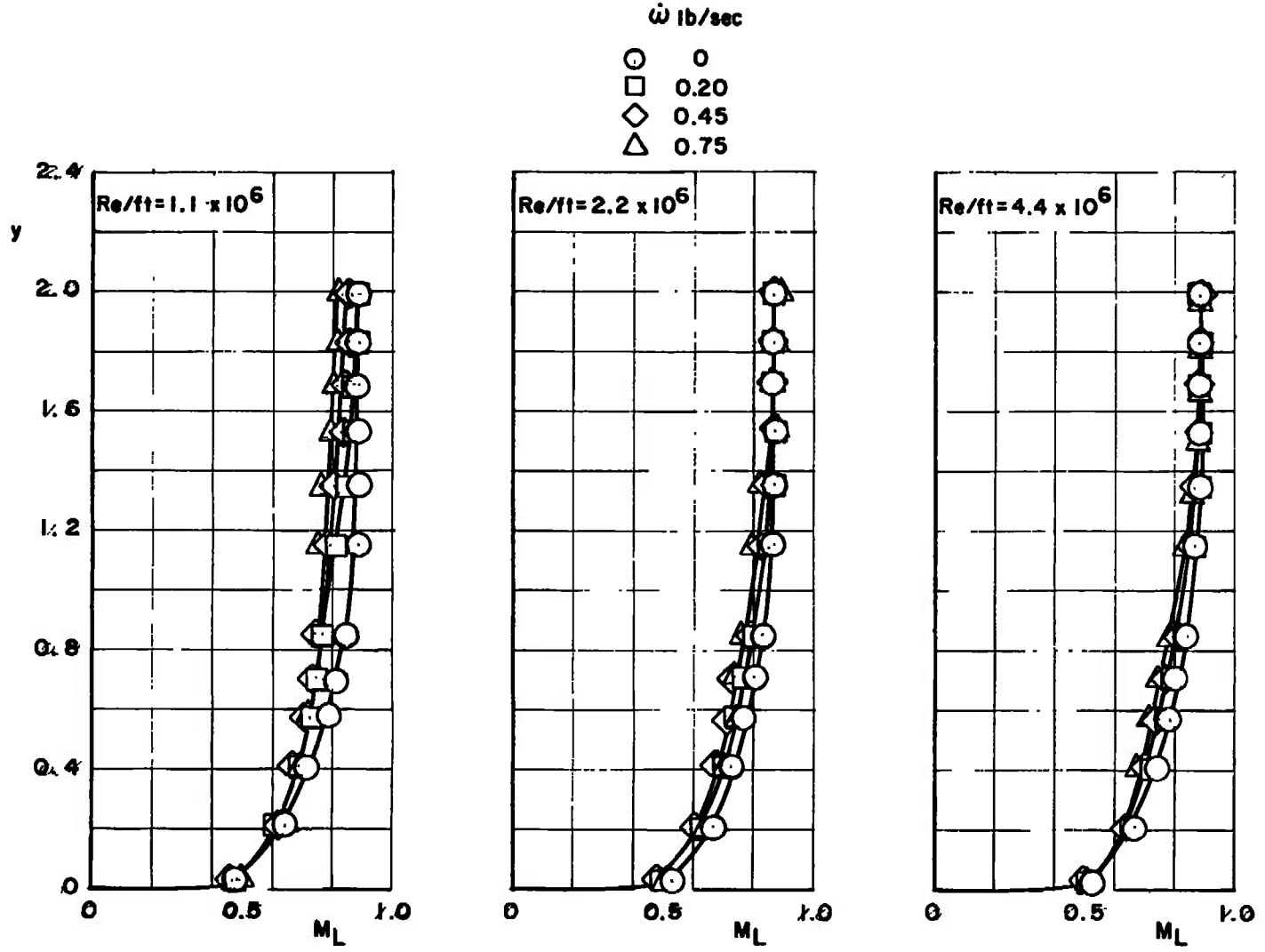

a. Mach Number 0.6

Fig. 10 Local Mach Number Profiles as a Function of Auxiliary Boundary-Layer Control Weight Flow

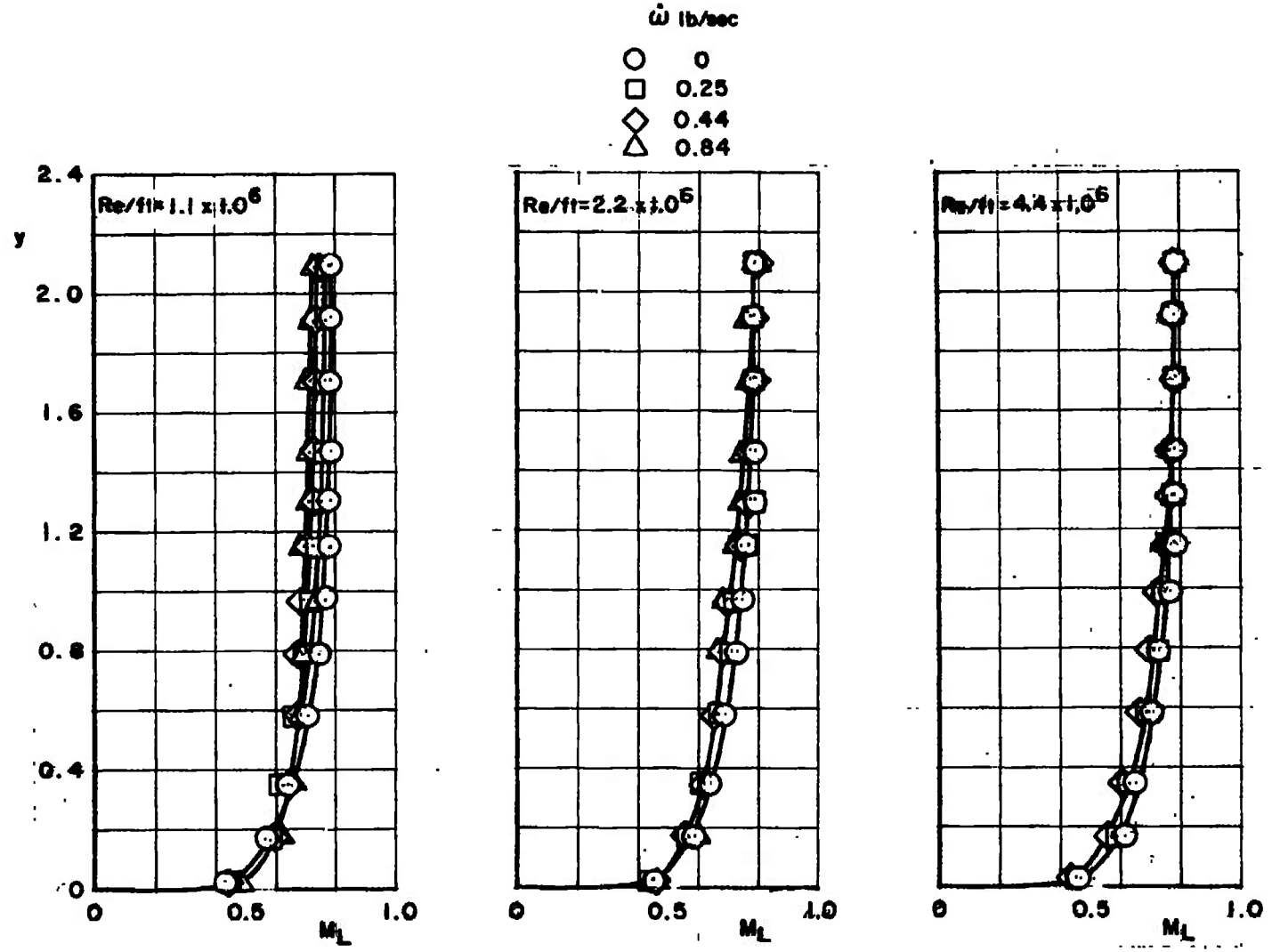

b. Mach Number 0.8
Fig. 10 Continued

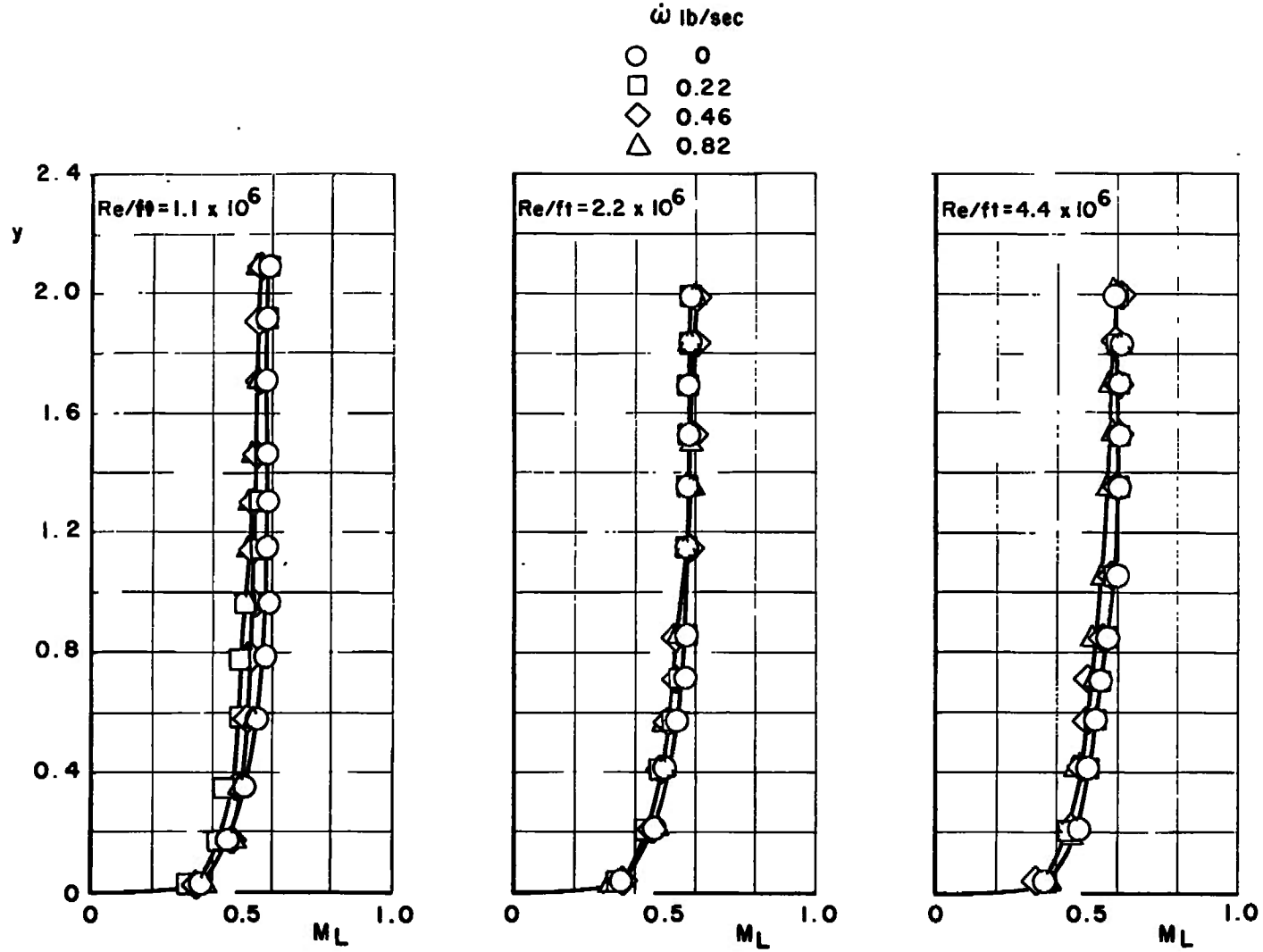

c. Mach Number 0.9
Fig. 10 Concluded

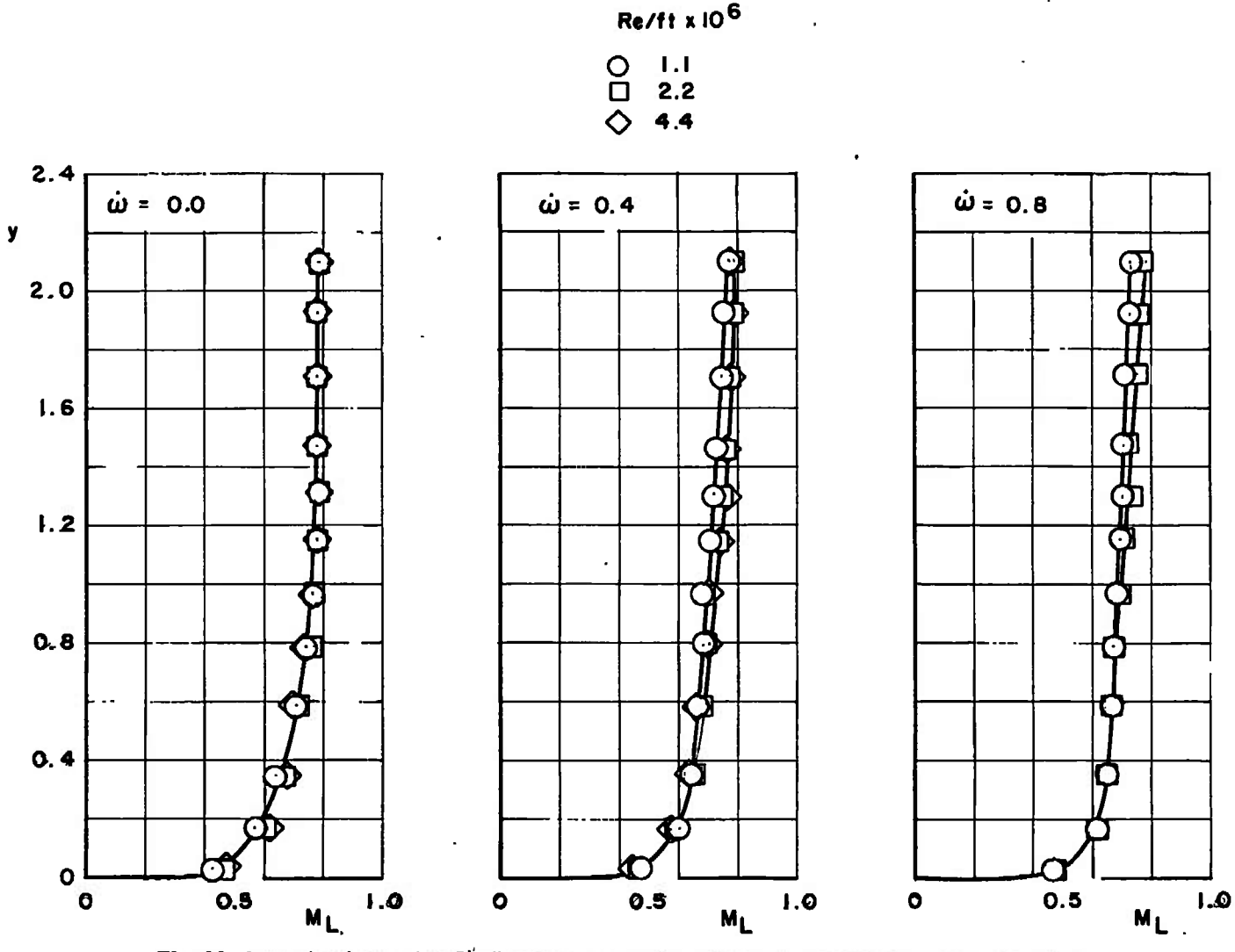

Fig. 11 Local Mach Number Profiles as a Function of Nominal Reynolds Number per Foot and Boundary-Layer Control Weight Flow

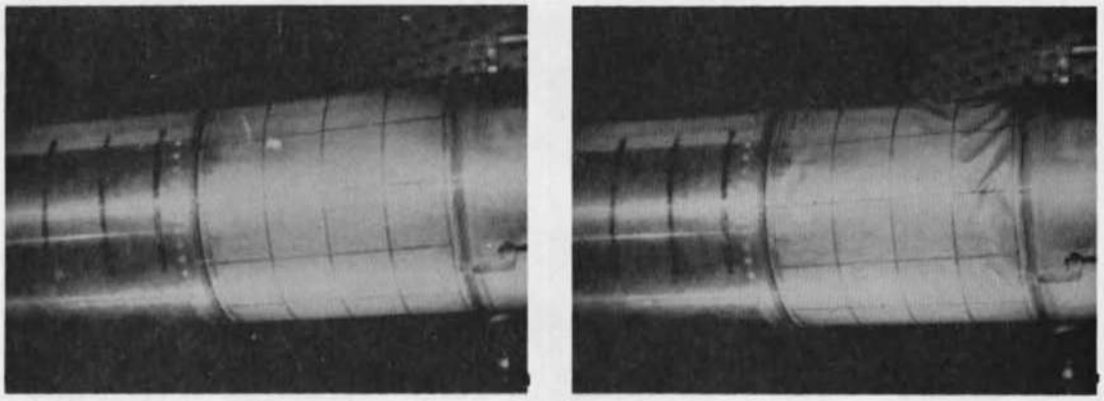

t = 0 sec

t = 0.02 sec

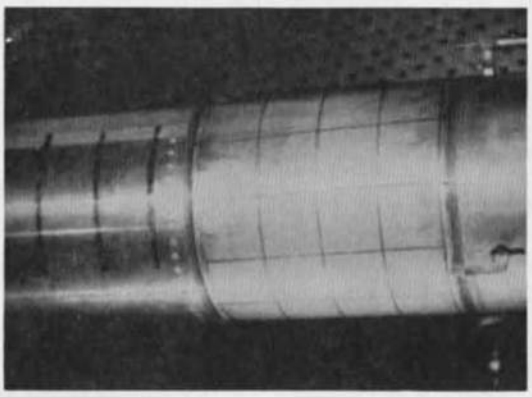

t = 0.005 sec

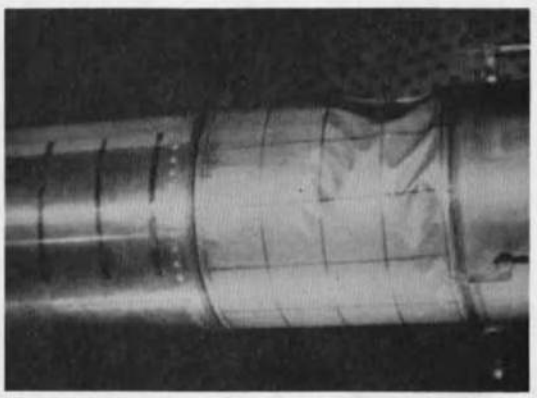

t = 0.03 sec

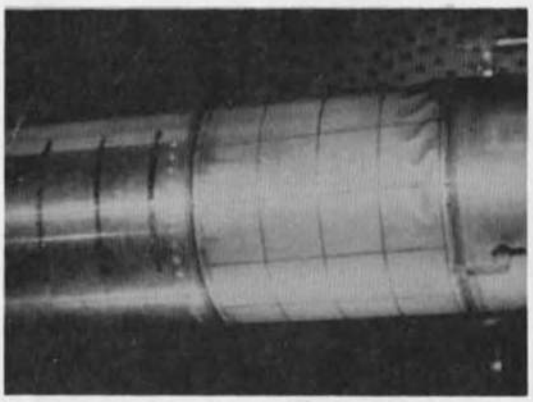

t = 0.01 sec

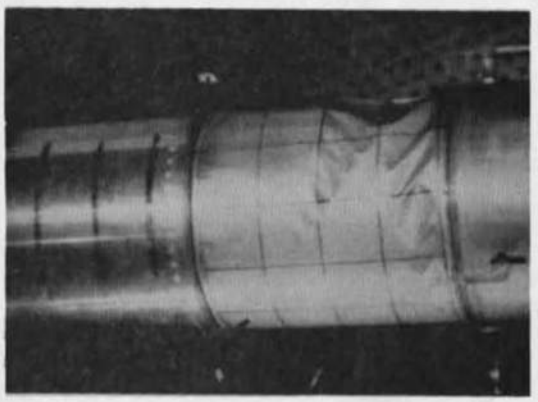

t = 0.04 sec

a. Configuration 1

Fig. 12 Sequence from High-Speed 16-mm Motion-Picture Film Illustrating Shell Static Aeroelastic Failure at M_∞ = 0.9

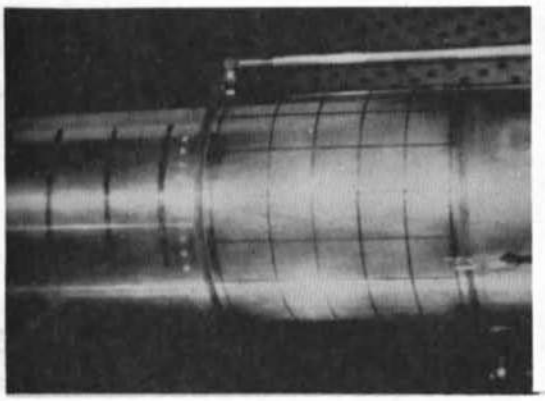

t = 0 sec

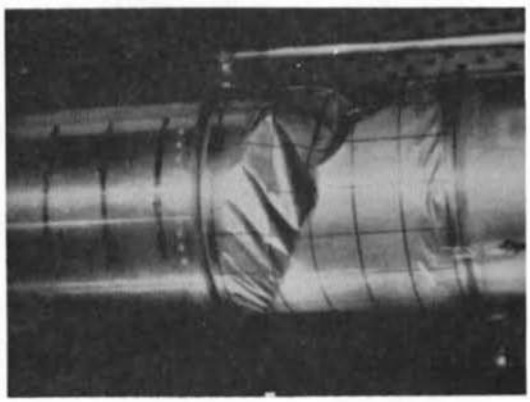

t = 0.05 sec

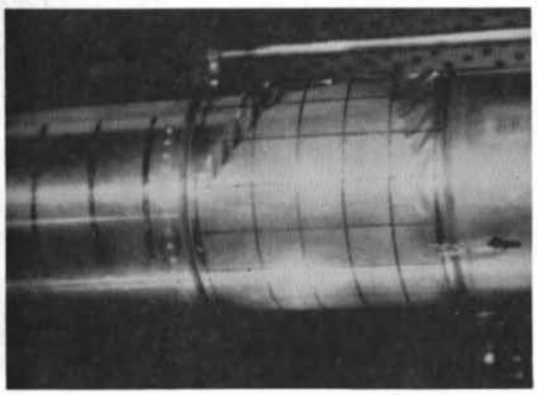

t = 0.02 sec

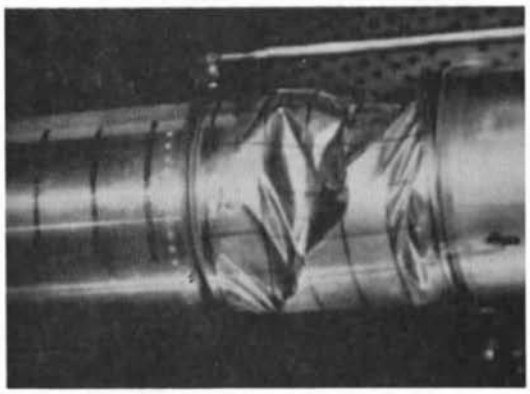

t = 0.06 sec

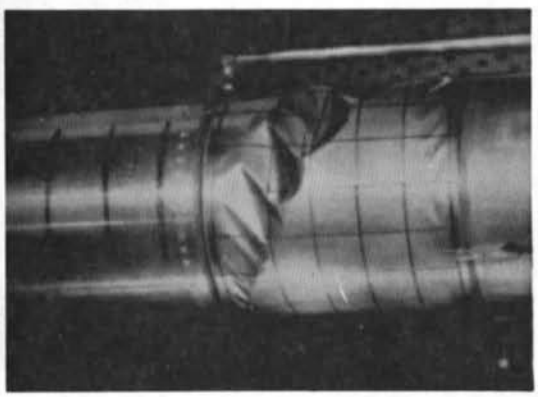

t = 0.04 sec

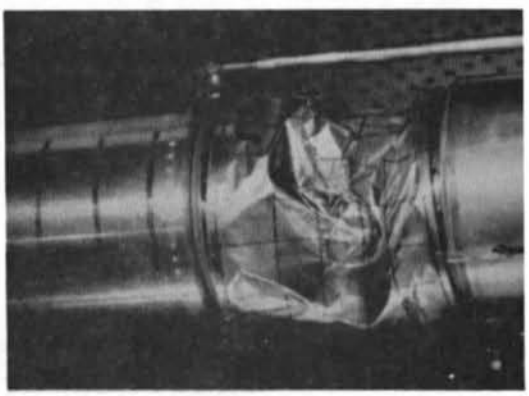

t = 0.07 sec

b. Configuration 3
Fig. 12 Concluded

TABLE I
SUMMARY OF TEST INFORMATION

Configuration	M_∞	p_{t_∞}, psfa	q_∞, psf	Re/ft x 10^6	$\overline{F}$	Δp_c, psi	p_a, psi	h, in.	$\dot{\omega}$, lb/sec	Remarks
3	0.90	2700	905	5.28	25.3	0.35	0	0.0030	0	Buckled
2	0.90	2700	905	5.28	25.3	1.35	0	0.0032	0	Buckled
1	0.90	2400	803	4.69	28.7	0.90	0	0.0027	0	Buckled

UNCLASSIFIED

Security Classification

DOCUMENT CONTROL DATA · R & D

(Security classification of title, body of abstract and indexing annotation must be entered when the overall report is classified)

1 ORIGINATING ACTIVITY (Corporate author)	2a. REPORT SECURITY CLASSIFICATION
Arnold Engineering Development Center Arnold Air Force Station, Tennessee 37355	UNCLASSIFIED
	2b. GROUP N/A

3 REPORT TITLE

INVESTIGATION OF THE AEROELASTIC STABILITY OF THIN CYLINDRICAL SHELLS AT SUBSONIC MACH NUMBERS

4. DESCRIPTIVE NOTES (Type of report and inclusive dates)

Final Report - May 5 through 9, 1971

5. AUTHOR(S) (First name, middle initial, last name)

Warren E. White, ARO, Inc.

6. REPORT DATE	7a. TOTAL NO. OF PAGES	7b. NO. OF REFS
November 1971	31	4

8a. CONTRACT OR GRANT NO	9a. ORIGINATOR'S REPORT NUMBER(S)
b. PROJECT NO.	AEDC-TR-71-173
c. Program Element 61102F/9F82 d. Task 01	9b. OTHER REPORT NO(S) (Any other numbers that may be assigned this report) ARO-PWT-TR-71-127

10. DISTRIBUTION STATEMENT

Approved for public release; distribution unlimited.

11. SUPPLEMENTARY NOTES	12. SPONSORING MILITARY ACTIVITY
Available in DDC.	Air Force Office of Scientific Research (NAM), 1400 Wilson Blvd., Arlington, VA 22209

13. ABSTRACT

Boundary-layer and static-pressure data were obtained over a rigid pressure shell at Mach numbers from 0.6 to 0.9 and Reynolds numbers per foot from 0.3×10^6 to 5.3×10^6. These data were obtained with and without the addition of air injected into the boundary layer through a circular slot upstream of the test shell. Static aeroelastic characteristics of thin cylindrical shells were obtained at Mach number 0.9 without the use of boundary-layer control and without shell axial-force loading. An aeroelastic buckling failure was induced on all three shells by reducing the cavity pressure. Flutter of the shell was not encountered during the test.

DD FORM 1 NOV 65 1473

UNCLASSIFIED

Security Classification

14. KEY WORDS	LINK A		LINK B		LINK C	
	ROLE	WT	ROLE	WT	ROLE	WT
cylindrical shells						
ogives						
aeroelasticity						
subsonic flow						
boundary layer						
static pressure						
buckling						

AFSC
Arnold AFS Tenn